


2013; Borstad et al., 2013; Hogg and Gudmundsson, 2017)). Studies by Jezek (1984); De Angelis and Skvarca (2003); Dupont and Alley (2005); Goldberg et al. (2009); Katz and Worster (2010); Gudmundsson (2013); Borstad et al. (2013) showed that increased calving can lead to destabilization of ice shelves and thus to a loss of the supporting mechanism (known as the “buttressing effect” or “back stress”) they provide to inland ice in Antarctica. This support can be crucial for the overall stability of the West Antarctic ice sheet as strong basal melting and reduced ice shelf buttressing can make the ice sheet unstable (Miles et al., 2013).


Developing a reliable calving law requires knowledge of where these fractures are located and how they evolve. Fractures in Antarctic ice shelves and the ice sheet are visible in satellite imagery, and can occur more often than every 50 m. Because of the size of Antarctica, the only feasible means of creating a data base of fractured zones is through the analysis of satellite imagery and altimetry. However, fractures can be covered by snow and/or not be visible because of poor resolution of the available imagery. It is for these reasons that inverse methods are often used (Borstad et al., 2013, 2016). Because of the incomplete knowledge of the location of fractured zones in Antarctica, models to represent fracturing in ice shelves/glaciers remain poorly constrained. The modelling of initiation and propagation of fractures is an active area of research, however no models to date have been able to successfully model this process on an ice-sheet scale. Existing studies have focused on Greenland (e.g. Nick et al. (2010); Cook et al. (2014); Krug et al. (2014); Sugiyama et al. (2015)), Svalbard (Chapuis and Tetzlaff, 2014) and the Antarctic Peninsula (e.g. Otero et al. (2010); Bassis and Walker (2012)) and a method that can universally describe calving at any ice shelf in Antarctica has not yet been developed.


The aim of this study is to construct an empirical model that can predict the locations of fractures. We focus on modelling of crevasses (surface fractures less than 200 metres wide) on the surface of the Antarctic ice sheet and surrounding ice shelves. Our model to predict fractured zones is based on a probabilistic approach, where we utilize the logistic regression algorithm (LRA) to find a relationship that enables the prediction of fracture locations. Our approach accounts for many potential parameters that include geometry, mechanical properties and flow regime (predictor parameters) and is based on a combination of modeling and remote sensing. We use a dataset of fracture observations, build by careful manual selection of the locations of visible fractures in satellite images, to build a model that can identify fractured regions on most of the Antarctic ice shelves as well as grounded ice regions around ice shelves in Antarctica, including the Antarctic Peninsula. We compare the ability of our model to match observations of fractures from satellite imagery versus the predictive ability of the damage-based method of Borstad et al. (2013). From the modelling of 45 ice shelves/glaciers, we found that we can predict the location of fractures that match the observations with a success rate ranging from ~45% to 99% (Figure 2a) for grounded ice and ~30% to 90% for floating ice (Figure 2a). The average success rate when applying damage method to floating ice was equal to 34% in contrast to 61% achieved when applying our LRA method. A mean over-estimation error of 26% and 20% for floating and grounded ice, respectively, occurs where we predict fractures in locations where no fractures are visible, but this may be affected by poor resolution of some of the satellite images and/or the presence of snow covering the surface of the ice. Our best results were achieved combining LRA with Bayesian as well as Jensen-Shannon Divergence theory described in Section 4.

Résumé des commentaires sur tc-2018-5-manuscript-version4.pdf

Page : 2

 Nombre : 1 Auteur : ogagliardini Sujet : Texte surligné Date : 25/08/2018 22:43:54
should read: (e.g. Nick et al., 2010; Cook et al., 2014; Krug...),

 Nombre : 2 Auteur : ogagliardini Sujet : Texte surligné Date : 25/08/2018 19:16:36

 Nombre : 3 Auteur : ogagliardini Sujet : Texte surligné Date : 25/08/2018 19:22:17

2 Background

2.1 Current state of calving computations in ice sheet models

A number of calving parameterisations have been developed and implemented in some software packages, but none of them includes the propagation of fractures both vertically and horizontally. Most of the available parameterisations are specific to a particular case and set of predictors (e.g. ¹Pralong and Funk, 2005), or calibrated for a particular location (e.g. Krug et al., 2014)), and therefore cannot be applied generically to any ice shelf.

²Discrete Element Models are used to predict short-term calving events ³HiDEM). Some other ice sheet models, such as ⁴ELMER/Ice, the Parallel Ice Sheet Model (PISM), the Community Ice Sheet Model (CISM) as well as the Ice Sheet System Model (ISSM), have attempted to include calving built on simplified physics (Alley et al., 2008). ⁵ISSM has a calving algorithm for marine terminating glaciers derived from a tensile Von Mises yield criterion (Morlighem et al., 2016). PISM uses a calving algorithm based on along- and across-flow strain rate (Levermann et al., 2012), which is based on the correlation between the calving rate and the first order approximation of local ice-flow spreading rate (it includes spreading rates of the first-order and assigns all higher order terms to zero). This idea is based on the observations of the increase of calving rate with along-flow ice shelf spreading rates and the spreading rates perpendicular to the calving front. However, it considers only large-scale behaviour and does not take into account the formation and propagation of crevasses. A second method implemented in PISM involves calculating a calving rate based on the critical ice thickness, which is mainly used to model calving of marine-terminating glaciers rather than floating ice shelves (due to different physics governing calving between the grounded ice and floating ice). Most of the experiments with ELMER/Ice calving were performed for Greenland glaciers, which have a different calving mechanism from the floating ice shelves in Antarctica (Van der Veen, 2002). The ⁶Community Ice Sheet Model (CISM) assumes that calving takes place when the water depth reaches a certain value (Price et al., 2014). This water-depth calving model uses flotation criteria to estimate the location of the glacier terminus. It allows calving to be linked to glacier dynamics as well as surface melting when applied to marine-terminating glaciers in Greenland (Nick et al., 2010). However, it cannot describe calving at floating ice shelves in Antarctica since the floating part is simply removed from the CISM model (the water-depth relationship requires a glacier to calve once it floats).

A number of other approaches have advanced our understanding of calving and the main existing studies are presented in Table 1. To date, Continuum Damage Mechanics (CDM) (Kachanov, 1958) and Linear Elastic Fracture Mechanics (Van der Veen, 1998a) are the most common methods used to model fractured zones, which is important information for modelling calving. The Linear Elastic Fracture Mechanics (LEFM) approach used by Krug et al. (2014) consists of calculating a stress intensity factor around fractures and assuming that they propagate until the factor falls below a certain critical value. To apply this method to any ice shelf, the modelled fractured zones need to be in good agreement with the observed surface fractures. Therefore, modelling the location of the fractured zones is an important basis for the subsequent estimation of fracture depth as well as calving and it must be described in the ice sheet models accurately. ⁷This method proposed Borstad et al. (2016) can describe both the formation and evolution of fractures in a fully viscous continuum damage model, although coupling with an elastic damage model might be more appropriate for representing short-timescale evolution of ⁸fractures. (Borstad et al., 2016).

1	Nombre : 1	Auteur : ogagliardini	Sujet : Texte surligné	Date : 25/08/2018 19:22:48
2	Nombre : 2	Auteur : ogagliardini	Sujet : Texte surligné	Date : 25/08/2018 23:07:24
This paragraph could be improved and reduced by avoinding first listing the model and then going into the description of each one.				
3	Nombre : 3	Auteur : ogagliardini	Sujet : Texte surligné	Date : 25/08/2018 19:24:55
give a paper reference not the name of a specific model				
4	Nombre : 4	Auteur : ogagliardini	Sujet : Texte surligné	Date : 25/08/2018 19:25:48
Elmer/Ice				
5	Nombre : 5	Auteur : ogagliardini	Sujet : Texte surligné	Date : 25/08/2018 19:26:37
.				
6	Nombre : 6	Auteur : ogagliardini	Sujet : Texte surligné	Date : 25/08/2018 19:27:27
already defined above				
7	Nombre : 7	Auteur : ogagliardini	Sujet : Texte surligné	Date : 25/08/2018 22:44:53
Which method are you referencing to? Not clear from the previous sentence.				
8	Nombre : 8	Auteur : ogagliardini	Sujet : Texte surligné	Date : 25/08/2018 19:29:44

¹Krug et al. (2014) built an alternative scheme by combining LEFM and CDM and found that they could match the observed evolution of a tidewater glacier in Greenland. This method is more complex compared to earlier approaches as it allows for both viscous and elastic behaviour and is able to reproduce development of small crevasses over a long period of time. The ELMER/Ice model (Gagliardini et al., 2013) combines CDM and LEFM to model calving, but this method has only been applied to Greenland (Krug et al., 2014). There are a number of studies that have proposed other calving laws (Pralong and Funk, 2005; Duddu and Waisman, 2012). These methods can include hydrofracture and other modes of failure, but have largely been applied to grounded calving margins, in contrast to the methods by Borstad et al. (2016) that are calibrated to remote sensing data and have been applied to ice shelves, but not grounded calving margins. Moreover, most of the mentioned methods ²might be not applicable in a generalised large-scale case.







10 3 ³Observational datasets

3.1 Ice Sheet System Model (ISSM) setup

Our statistical model is built upon knowledge of the velocities, stresses, strain rates, back stresses as well as friction coefficient and viscosity of the ice. We use ISSM (Larour et al., 2012) to derive estimates of these predictors for our statistical model. ISSM is a fully dynamic model that includes both two dimensional (2-D) and 3-D stress balance approximations. Our experiments rely on the shelfy stream approximation (SSA) as it is computationally cheap and suitable for modelling floating ice shelves and grounded ice streams undergoing widespread basal sliding.

All our experiments were performed for 45 ice shelf regions in Antarctica (see Figure 3a), each including both ice shelves and the grounded ice ⁴around 100 kilometres upstream from the grounding line (hereafter referred to as ice shelf regions or ice shelf/glacier). We ran one simulation to create a stress balance solution per region (ice shelf/glacier), which allowed us to obtain the predictor parameters required for the calculation of the probability of fracturing. We used SeaRISE air temperature, snow accumulation and geothermal heat flux (Le Brocq et al., 2010) as climate forcing data. The information about the ice temperature for grounded ice is calculate as the depth-average temperature from Liefveringe and Pattyn (2013); Pattyn (2010) (21 vertical levels). The steady-state depth averaged ice temperature on floating ice shelves (mainly used for the calculation of damage) was calculated using surface, basal temperatures and basal melting rate according to Holland and Jenkins (1999). To calculate ice temperature we corrected the surface temperature with a lapse rate and imposed it on the ice surface. Basal melting rates on ice shelves were taken ⁵from (Depoorter et al., 2013).

The data for the geometry of the ice shelves and surrounded grounded ice (bedrock topography, ice thickness and glacier surface) were interpolated from Bedmap2 data (Fretwell et al., 2013) at 1 km spatial resolution. Basal friction under grounded ice and rheology for floating ice were calculated from an inversion of velocities (Khazendar et al., 2007), where the observations of the horizontal ice velocities were taken from InSAR (450-metres resolution) (Rignot et al., 2011b, a) and the sliding law is the Budd sliding law (Budd et al., 1979). In the inversions we used regularisation to penalise sharp gradients of the cost function, calibrated using an L-curve analysis (Morlighem et al., 2013). We set boundary conditions as follows: the upper surface is considered stress-free and friction is applied at the ice-bedrock interface. ⁶At the inflow boundary we applied Dirichlet

 Nombre : 1	Auteur : ogagliardini	Sujet : Texte surligné	Date : 25/08/2018 19:30:33
<hr/>			
 Nombre : 2	Auteur : ogagliardini	Sujet : Texte surligné	Date : 25/08/2018 19:32:03
<hr/>			
 Nombre : 3	Auteur : ogagliardini	Sujet : Texte surligné	Date : 25/08/2018 19:33:56
<hr/>			
 Nombre : 4	Auteur : ogagliardini	Sujet : Texte surligné	Date : 25/08/2018 19:34:10
<hr/>			
 Nombre : 5	Auteur : ogagliardini	Sujet : Texte surligné	Date : 25/08/2018 19:35:29
<hr/>			
 Nombre : 6	Auteur : ogagliardini	Sujet : Texte surligné	Date : 25/08/2018 19:36:54

conditions. The position of the grounding line position is calculated using a flotation criterion. **We used the outputs of the simulations as input for our modelling using ISSM** and as the predictor factors in our probabilistic method (see Section 4.1).

For all the simulations, we used a multi-resolution mesh approach for the chosen domains in East and West Antarctica as well as the Antarctic Peninsula. This method was chosen due to the fact that on the one hand using a 50- or 100-metre mesh resolution created a significant increase in the computational time of the model, but on the other hand it was important to have a fine resolution mesh in order to model surface fractures, as the distance between them is normally around 50-100 metres. In order to have a fine resolution together with smaller computational time, we first calculated all the main predictors on a 200-metre resolution mesh (to achieve a faster computational speed) and then interpolated the values to nodes on a 100-metre resolution mesh (to use in our fracture model resolved at 100-metres). All further computations and analyses were performed on this finer mesh.

3.2 Observing fractures using satellite images

We focus only on predicting the location of surface crevasses without modelling rifts, since the processes that cause rift opening might differ from processes that allow surface crevasses to stay open. In fact rifts might be formed due to presence of basal fractures, tidal deformation (Bromirski et al., 2010), ocean swell (Bassis and Walker, 2012) and stay open due to presence of melange (mix of snow and sea ice) (Rignot and MacAyeal, 1998; Larour et al., 2004; Bassis et al., 2005; Fricker et al., 2005). To model this we would need to include information about ocean temperature, sea ice and seismic activity, all of which is outside the scope of this paper. Moreover, rifts form when cracks propagate through the entire ice thickness and, therefore, the ice becomes effectively discontinuous. We, therefore, do not include rifts and focus only on surface crevasses.

In order to obtain the observations of the location of fractures on the ice sheet surface we used satellite images taken from Google Earth-Pro, where images of the Antarctic ice sheet were available at different spatial resolutions. However, to be able to see surface fractures we limited our choice to only images with a horizontal resolution smaller than 10 metres for the period between 2011 and 2015. We included only regions with at least one high resolution satellite image and where it was relatively easy to identify surface fractures.

The visual images of the ice surface include many features and it is important to distinguish the surface fractures from other patterns such as surface troughs (formed as a result of presence of bottom crevasses or subglacial channels). It has been suggested by Luckman et al. (2012) that wide features on the images with a large spacing between them (e.g > 1 km) are more likely to be troughs associated with basal crevasses. Modelling of basal fractures is outside the scope of this papers. Thus, such large linear features that are visible on the satellite images are surface troughs and should not be interpreted as surface fractures that our model fails to predict.

To construct a set of observed fractures, we manually selected fractured locations as well as non-fractured zones that we could identify in the satellite images. Most of the identified non-fractured regions are located in blue ice regions, which are areas with low snow accumulation or where the snow has been removed by the wind. In such areas we can clearly see where the ice is not damaged. It is important to note that in some locations the resolution of images was not always sufficiently high

output of which simulations. I only see ISSM simulations in what is above?

to clearly see every fracture. Moreover, some surface fractures may be covered in snow and, therefore, are not identified by our analysis.

We constructed two different types of data sets: ‘calibration’ and ‘evaluation’, for building the statistical model and for studying the output of the model, respectively.

5 In the calibration data set we select a subset of observed fractures, being a representative sample of locations where fractures are found on 35 ice shelves/glaciers. The statistical approach requires training on a large number of ice shelf regions with different characteristics and a variety of observations. Therefore, we use our calibration dataset to train our LRA. This improves the reliability of the model, as the diversity in sampling provides a better estimation of correlation coefficients (called β coefficients in LRA). We assign a value of 1 to fractured nodes and 0 to non-fractured nodes (due to the fact that **1 Logistic**
10 Regression Analysis (LRA) that we use in our approach, described later in section 4.1 uses a categorical input).

We form the evaluation data set to test how well our new approach predicts fractures for each ice shelf region individually. Although we did not need to select all the fractures on the ice sheet surface to build the calibration data set, to construct the evaluation data set we made a concerted effort to select the majority of the visible surface fractures on each of the ice shelf regions. It is possible that some fractures were missed due to the large spatial extent of the experiments. Moreover, we do
15 not present every fracture on the figures in this paper in order to make the figures legible. In addition, we perform validation experiments with another 10 ice shelf regions to test how well LRA works for a randomly selected ice shelf/glacier that was not a part of the construction of the model.

It is important to note that the evaluation data sets are not just discrete values (0 and 1), but are a continuous field representing the probability of observing a fracture in a location. In a node where we could see a fracture we assigned the probability of
20 observing a fracture to 1. Nodes around the observed fracture are more likely than not to be fractured. It is important to mention that the spacing of crevasses is often linked to their depth. A single crevasse can penetrate much deeper than a crevasse in a set of closely spaced crevasses. However, in this study we do not focus on estimating either depth or spacing of crevasses. Therefore, we then set the probability of observing a fracture to simply decrease from 1 to 0.55, decreasing with increased distance from the observed fracture (within 500 metres radius). On the other hand, if a non-fractured node was found within
25 a region with high resolution imagery, we assigned the probability of fracturing in this node to 0.05. Within a 500 metres radius of the non-fractured node we allowed the probability to increase linearly from 0.05 to 0.4. In all other nodes we set the probability of observing a fracture to 0.5. The last assumption is due to the fact if there are no fractures visible in the area of poor resolution of the image it is equally likely for the node to be fractured or non-fractured. This allows us to account for uncertainties of the observations, since it is not always possible to determine whether there are no fractures or whether fractures
30 are just not visible. We do not include any information about the depth and spacing of the crevasses.

4 Methods

We used statistics-based methods as an alternative to physics-based approaches in order to gain insights into the location of fractured zones in ice shelves and glaciers. In the well-known damage-based approach, the damage variable varies from 0 to 1

why a new definition of LRA here?


representing the fraction of a volume that is fractured, with 0 being not fractured and 1 being fully fractured. Instead of using damage-based method we use the **Logistic Regression Algorithm (LRA)**, which provides us with the probability of fracturing (also varying from 0 to 1). We then apply this method to derive fracture likelihood functions for both floating ice shelves and the grounded ice for any ice shelf region. To construct the likelihood function we need to find coefficients that describe the relationships between predictor variables and what we want to predict (in our case it is surface fractures not including rifts). Thus, in order to create a statistical model we use our calibration data set of observations of surface fractures and non-fractures as well as information about the flow regime at the locations of each observation (predictor parameters).


Our main goal is to determine the most likely location of surface fractures. We do not focus on identifying the location of their initiation, since it is not possible to know whether the observed fractures were formed where observed or have advected to that position having formed upstream. We tried to select observed fractures where there were no other fractures visible upstream, meaning that the observed fractures would identify the initiation zones, but this may not always be possible. The model will, therefore, predict the locations of initiation of fractures but also some zones to which fractures have advected. For this reason, we do not distinguish between the high-advection (advection from upstream) and low-advection (because of local stresses) (Colgan et al., 2016) **cycles**. Although we do not directly model advection, the statistical model predicts the presence of both initiated and advected fractures without distinguishing one from another. The question that arises then is how do we know that the flow regime conditions that caused opening of the fracture are the conditions at the point where the fracture is observed and not the conditions upstream from the observed fracture (in case of advection)? However, even if an observed fracture was not formed at a particular location, but was advected with the ice flow, it is still visible on the satellite image. The fact that fractures can be seen indicates that there are factors at that location that act to permit the fractures to exist, whether they formed in that particular location or remained open after being advected from upstream (since another combination of factors could close the fracture).

This section is structured in the following order. First, we present our method (logistic regression algorithm) used for predicting the formation of fractures. Second, we describe the predictor factors (predictors) we include in this method. Then, two methods used for optimising a set of predictor factors are presented (Bayesian based algorithm and Jensen-Shannon Divergence). Finally, we present the damage calculation used for a qualitative comparison with our results.

4.1 The logistic regression algorithm (LRA)

Logistic regression is a statistical technique generally used to classify data based on values of input fields. The method is similar to linear regression but takes a categorical target field (in our case nodes which are fractured or non-fractured) instead of a numerical series. The logistic function allows us to calculate the likelihood of an event as a function of different predictor factors (see Table 2 for the predictors used in our model). Taking any range of data, it produces values from 0 to 1 and thus it can be used to represent the probability of fracturing (Hosmer Jr and Lemeshow, 2004).

 Nombre : 1 Auteur : ogagliardini Sujet : Texte surligné Date : 25/08/2018 19:48:43
again

 Nombre : 2 Auteur : ogagliardini Sujet : Texte surligné Date : 25/08/2018 19:50:33
before the ref

To apply the logistic regression algorithm, we constructed a logistic function P_j (Eq. 1) that describes the probability of a certain node to be fractured as a function of the predictor factors x_i . This function is not designed to provide any information about the depth of a fracture, just its spatial location.

$$P_j = Prob(X = 1|x_i) = \frac{\exp(\beta_0 + \beta_1 \cdot x_{1j} + \beta_2 \cdot x_{2j} + \beta_3 \cdot x_{3j} + \dots)}{1 + \exp(\beta_0 + \beta_1 \cdot x_{1j} + \beta_2 \cdot x_{2j} + \beta_3 \cdot x_{3j} + \dots)}, \quad (1)$$

5 **1** here for j is the node number, x_{ij} is the value of predictor x_i for node j and β are correlation coefficients. The unknown coefficients β_i are found by maximising the likelihood function L (Eq. 2) **2**

$$L(\beta_j) = \prod_{j=1}^n P_j^{\delta_j} (1 - P_j)^{1 - \delta_j}, \quad (2)$$

where n is the number of observations and δ is the Kronecker symbol:

$$10 \quad \delta = \begin{cases} 1, & \text{when there is a surface fracture visible on a satellite image} \\ 0, & \text{otherwise.} \end{cases} \quad (3)$$


Once the values of β are found we can find the probability of a node to be fractured by substituting a chosen set of predictors into **3** equation 1.


4.2 Predictor parameters:


We started with a set of 19 predictors, x_i . Some of them are known to influence fracturing (stresses, strain rates, ice rheology), while others we considered to be potentially important (various geometrical properties, proximity to the ice front and the grounding line, etc). Temperature and accumulation were not included in the list of predictors due to the incompatibility of their spatial resolution with the relatively fine 100-metre mesh we used to model fractures. They might be important for the formation and propagation of fractures, as warmer temperatures can increase the number of fractures due to the effect of melt water (Weertman, 1973; Van der Veen, 1998b; Mobasher et al., 2016), but a better resolution climate dataset would be needed to assess this.

All the experiments and sets of parameters used in LRA were constructed separately for floating and grounded ice. This is due to the fact that some parameters that were used for prediction of fractures on grounded ice are not applicable for predicting fractures on floating ice and vice versa (for example, friction and bed slope are irrelevant on floating ice, whereas back stress cannot be applied to grounded ice).

25 The calculation of some predictors was performed using methods already implemented in ISSM (e.g. stresses, strain rates, friction coefficient). Other predictors (e.g. calculation of curvature, distances to ice front, grounding line, proximity to glacier edges and nunataks) are not produced by ISSM and were calculated independently. Here we describe the methods we used to

 Nombre : 1 Auteur : ogagliardini Sujet : Texte surligné Date : 25/08/2018 19:53:40
where j is ?

 Nombre : 2 Auteur : ogagliardini Sujet : Texte surligné Date : 25/08/2018 19:53:44
:

 Nombre : 3 Auteur : ogagliardini Sujet : Texte surligné Date : 25/08/2018 19:54:23

calculate each predictor parameter as well as a brief description as to why each parameter may have an impact on the location of fractures:

(i) Principal values of the deviatoric stress and effective stress:

Following the Shallow ice approximation, the deviatoric stress is:

$$5 \quad \sigma' = \begin{bmatrix} \sigma'_{xx} & \sigma'_{xy} & 0 \\ \sigma'_{xy} & \sigma'_{yy} & 0 \\ 0 & 0 & -\sigma'_{xx} - \sigma'_{yy} \end{bmatrix} \quad (4)$$

The deviatoric stress values have a direct effect on the opening and closing of crevasses; the sign of the first principal stress component determines whether it is compressive (negative) or tensile (positive). Effective deviatoric stress is calculated as:

$$\sigma'_e = \sqrt{\sigma'^2_{xx} + \sigma'^2_{yy} + \sigma'^2_{xy} + \sigma'_{xx}\sigma'_{yy}}, \quad (5)$$

10 **1** here σ'_{ij} are the deviatoric stress components.

Von Mises stress is calculated as:

$$\sigma_{vm} = \sqrt{\frac{3}{2} \sum_{i,j} \sigma'_{ij} \sigma'_{ij}} = \sqrt{3B} \dot{\epsilon}_e^{1/n} \quad (6)$$


where B and n are the creep parameter and the creep **2** exponent, respectively.


(ii) Effective strain rate:

15 The effective strain rate $\dot{\epsilon}_e$ is included in our analysis because it is known that crevasse initiation is linked to strain rates (Campbell et al., 2013). If the strain rate in the horizontal plane is sufficiently high, crevasses can propagate to greater depth (Benn and Evans, 2010). In addition, stresses can trigger brittle fracturing but, to take into account a gradual viscoelastic effect that can lead to fracture formation, strain rates are included in our model.

The principal strain rates are calculated as eigenvalues of the matrix:

$$20 \quad \dot{\epsilon} = \begin{bmatrix} \frac{\partial u}{\partial x} & \frac{1}{2} \left(\frac{\partial u}{\partial y} + \frac{\partial v}{\partial x} \right) & 0 \\ \frac{1}{2} \left(\frac{\partial u}{\partial y} + \frac{\partial v}{\partial x} \right) & \frac{\partial v}{\partial y} & 0 \\ 0 & 0 & -\frac{\partial u}{\partial x} - \frac{\partial v}{\partial y} \end{bmatrix} \quad (7)$$

 Nombre : 1 Auteur : ogagliardini Sujet : Texte surligné Date : 25/08/2018 19:57:46
should be below Eq. (4)

 Nombre : 2 Auteur : ogagliardini Sujet : Texte surligné Date : 25/08/2018 19:58:21
and what is ϵ ?

where u and v are horizontal components of the surface velocity.

Using again the shallow ice approximation, vertical shear is neglected and the **1** effective pressure is approximated as:

$$\dot{\epsilon}_e = \sqrt{\dot{\epsilon}_{xx}^2 + \dot{\epsilon}_{yy}^2 + \dot{\epsilon}_{xy}^2 + \dot{\epsilon}_{xx}\dot{\epsilon}_{yy}}, \quad (8)$$

5 where $\dot{\epsilon}_{ij}$ are the strain rate components (since in 2D we neglect $\dot{\epsilon}_{xz}$ and $\dot{\epsilon}_{yz}$ and using incompressibility $\dot{\epsilon}_{zz} = -\dot{\epsilon}_{yy} - \dot{\epsilon}_{xx}$).

(iii) Horizontal strain rate gradient:

10 The change in strain rate sometimes is not the cause but the consequence of the presence of fractures. However, the aim of our study is to identify where fractures are present without attempting to fully describe the process by which they are formed. Thus, we use the change in strain rate as a predictor precisely because it tells us where we can expect to find fractures. This predictor allows us to discover new regions where crevasses are present even if they were not seen in the imagery. A lack of observed fractures but high strain rate means **2** that fractures may not be visible but should still be present (e.g. if fractures are covered in snow or not visible due to bad resolution of the satellite images). Furthermore, changing geometry or boundary conditions can cause changes in strain rate, and also cause fractures (e.g. a glacier flowing over a convex slope or icefall: the change in bed slope causes a change in strain rate and also causes fractures, **3** and it's not the fractures that cause the change in strain rate in this case.

(iv) Friction:

Low friction at the base of glaciers will lead to a higher sensitivity to membrane stresses, which can lead to more crevassing in tensile mode. **4** We obtain this parameter from the inversion of surface velocities in ISSM.

(v) Stiffness of ice and **5** ice **6** thickness:

20 In addition, we include the viscosity parameter B in Glen's flow law as well as ice thickness **7** due to their physical relation to fracture mechanics. When ice stiffness increases and ice crystals cannot creep fast enough, fracture may occur. Therefore, this parameter (obtained from the inversion of velocities implemented in ISSM) is added as a predictor. Adding temperature directly into the analysis did not improve the prediction results, which might be due to the uncertainties in the temperature estimation.

25 (vi) Proximity to glacier edges:

30 Generally the lateral friction along the glacier boundary is not considered in ice sheet models when stress is calculated. The stress field alone can predict transverse, longitudinal and radial splaying crevasses. They are all formed due to opening stress and are normally considered in existing damage modelling methods. However, the prediction of crevasses near the edges of glaciers requires a parameterisation of the lateral drag. Thus, we include the proximity to edges of glaciers and to nunataks as a predictor in our model.

T Nombre : 1 Auteur : ogagliardini Sujet : Texte surligné Date : 25/08/2018 19:59:35
effective strain-rate

T Nombre : 2 Auteur : ogagliardini Sujet : Texte surligné Date : 25/08/2018 20:01:53
or not. It can also be badly estimated from error in the velocity field?

T Nombre : 3 Auteur : ogagliardini Sujet : Texte surligné Date : 25/08/2018 20:03:50
I don't agree with this, and it is in contradiction with what is written just before. Yes, at the end, it is the strain rate that will cause the fracture to open, because of a particular bedrock geometry

T Nombre : 4 Auteur : ogagliardini Sujet : Texte surligné Date : 25/08/2018 20:05:07
the same should be tell for all parameters.

My feeling is that stress and strain rate parameters are obtained from the same observation, eg surface velocity? This should be clearly mentioned.

T Nombre : 5 Auteur : ogagliardini Sujet : Texte surligné Date : 25/08/2018 20:07:42
why ice thickness here? It is not mentioned in the following paragraph

T Nombre : 6 Auteur : ogagliardini Sujet : Texte surligné Date : 25/08/2018 20:06:32

T Nombre : 7 Auteur : ogagliardini Sujet : Texte surligné Date : 25/08/2018 20:08:15
which I cannot see. Should be explained

(vii) Distance to the ice front and the grounding line:

¹We can see in the satellite images that more fractures are present at a certain distance from the ice front as well as near the grounding line. We found that the relation between the presence of fractures and distance to the ice front as well as the distance to the grounding line is non-linear (Figure 3b). For most ice shelves/glaciers we can see more fractures 3-5 km as well as 10-13 km away from the front and a slightly smaller number of fractures closer than 3 km to the front or between 5 and 10 km. Therefore, instead of using d_{IF} and d_{GL} (distance to the ice front and the grounding line in km) as predictor variables, we construct dummy variables: DM_{IF} and DM_{GL} , respectively, which represent two-column arrays in the following form:

$$DM_{IF} = \begin{cases} (1, 1), & \text{when } 3\text{km} \leq d_{IF} < 5\text{km} \\ & \text{or } 10\text{km} \leq d_{IF} < 13\text{km} \\ (1, 0), & \text{when } 5\text{km} \leq d_{IF} < 10\text{km} \\ (0, 1), & \text{when } d_{IF} < 3\text{km} \\ (0, 0), & \text{else} \end{cases} \quad (9)$$

$$DM_{GL} = \begin{cases} (1, 1), & \text{when } 5\text{km} \leq d_{GL} < 15\text{km} \\ (1, 0), & \text{when } d_{GL} < 5\text{km} \\ (0, 1), & \text{when } 15\text{km} \leq d_{GL} < 20\text{km} \\ (0, 0), & \text{else} \end{cases} \quad (10)$$

(viii) Bed and surface slopes:





²There are a number of parameters such as surface velocity, surface slope and a curvature of a glacier channel that are included by other studies in the calculation of the stress field (Larour et al., 2012), but for our method we look at each component separately:

Thus, bed and surface slopes are included in the ³model since shear stress increases on a steeper slope and can lead to fracturing (e.g. ice fall is an extreme case).

(ix) Surface gradient change:

We include this predictor in the analysis due to the fact that fracturing can be caused by ⁴an increase in stress due to an abrupt change in surface elevation.

(x) Curvature:

-
-  Nombre : 1 Auteur : ogagliardini Sujet : Texte surligné Date : 25/08/2018 20:12:07
you might capture them in the stress field with a FS model. It should be discussed that the fact that you don't capture them directly with stress is because of the SSA assumption.
-
-  Nombre : 2 Auteur : ogagliardini Sujet : Texte surligné Date : 25/08/2018 20:12:58
I don't understand what you mean here
-
-  Nombre : 3 Auteur : ogagliardini Sujet : Texte surligné Date : 25/08/2018 20:13:42
and why it doesn't appear in your stress field?
-
-  Nombre : 4 Auteur : ogagliardini Sujet : Texte surligné Date : 25/08/2018 20:14:13
then is should be seen in the stress field?

It is clearly visible in satellite images that more fractures occur around horizontal bends in glaciers. Therefore, the curvature of the glacier channel was included as a predictor, calculated as:

$$\alpha = \arccos\left(\frac{\mathbf{v}(P) \cdot \mathbf{v}(E)}{|\mathbf{v}(P)| \cdot |\mathbf{v}(E)|}\right), \quad (11)$$

where $\mathbf{v}(P)$ is the ice velocity at the point of observations and $\mathbf{v}(E)$ is the velocity D metres away from the point. The distance D is based on the velocity magnitude $\mathbf{v}(P)$, because if the velocity is high we need to increase D so that two subsequent points capture the geometry of the bend of a glacier. Thus, if $\mathbf{v}(P)$ is greater than 2000 m/yr we assign $D = 3\mathbf{v}(P)$, otherwise $D = 6\mathbf{v}(P)$. These values are not arbitrary: this assignment is used in the model only to have enough data points to see the local curvature of a glacier and it does not affect the calculation of the curvature itself.

Finally, due to the fact that all predictor parameters have different units, as well as significantly different magnitudes, we normalise each predictor as following:







$$x_i^* = \frac{x_i - \mu_i}{\sigma_i}, \quad \text{where } \mu_i \text{ and } \sigma_i \text{ are mean and standard deviation of the predictor variables, respectively.} \quad (12)$$

4.2.1 Test run with a small set of parameters

Including stress variables to predict fractures is intuitive as they are one of the major indicator of ice been fractured or non-fractured. Other variables such as geometry correlate to stress variables, but we found that it is important to include them in the model because the results are inferior if the parameters are not included. This might be caused by limitations of the predictor parameter values produced by the ice sheet model.

In order to show that our fracture model works better when including both physics-based and geometry-based predictors, we ran three additional experiments. In the first test run we included only effective deviatoric stress as a predictor and found that, although it produces reasonable results matching the observations, the success of identifying fractures is about 30 per cent lower than the results of the model with the chosen optimal set of the predictors (Figure 1 (a,b)). The second set of experiments contained only principal stresses and produced results that did not agree well with the observations (Figure 1 (c,d)). Similarly, the results of the third test, that included only von Mises stress as the predictor, did not agree with the observed fractures (success rate not exceeding 40 per cent, Figure 1 (e,f)). This shows that stress measures alone are not sufficient to model fractured zones and a more complex set of predictor parameters is required.

Moreover, including both friction and strain rate might be ambiguous since lower friction can lead to larger strain rate. By looking at the predictor data sets we found that the optimal choice of parameters for each group includes either friction or strain rate, never both at the same time. We ran an experiment replacing strain rates by friction and found that the prediction success for some glacier decreases by only about 3%. We, therefore kept only strain rate as a predictor parameter and discarded friction.

	Nombre : 1	Auteur : ogagliardini	Sujet : Texte surligné	Date : 25/08/2018 22:53:17
is it x_i^* or x_i which is used in Eq. (1)? This should be mentioned.				
	Nombre : 2	Auteur : ogagliardini	Sujet : Texte surligné	Date : 25/08/2018 20:16:37
more than the ice sheet model, it is the simplification of the Stokes equation that might explain this.				
	Nombre : 3	Auteur : ogagliardini	Sujet : Texte surligné	Date : 25/08/2018 20:17:24
20%				
	Nombre : 4	Auteur : ogagliardini	Sujet : Texte surligné	Date : 25/08/2018 20:17:32
50%				
	Nombre : 5	Auteur : ogagliardini	Sujet : Texte surligné	Date : 25/08/2018 20:19:02
this is not a stress measure, but a velocity measurement converted in stress through a model relying on SSA.				
	Nombre : 6	Auteur : ogagliardini	Sujet : Texte surligné	Date : 25/08/2018 20:21:00
delete				

$$\phi_d(m) = \frac{(E(f_i^{obs}) - E(f_d^{pred}))^2}{\sigma^2}. \quad (20)$$

We performed a Bayesian analysis for 500 steps, then narrowed down the selection and accepted only those models that had likelihoods greater than 90% of the best likelihood. Each step included two criteria: if a new likelihood was greater than the prior likelihood or was greater than a certain percentage (taken at random at each step) of the old likelihood we accepted the model. This allowed us to identify the most commonly chosen sets of parameters.

4.4 Glaciers classification and Jensen-Shannon Divergence (JSD)

In order to select a set of predictors for a general case and to find whether it is possible to identify a set that can be used for any ice shelf region, we started with the construction of a binary array for each ice shelf/glacier, where the number of rows represents the number of good-fitting models for an ice shelf/glacier and the number of columns represents each of the predictor factors.

We then found the average occurrence of each predictor:

$$A_i = \frac{1}{N} \sum_{j=1}^N k_j, \quad (21)$$

where $i \in [1, 17]$ is the predictor index, N is the number of good-fitting models. $k_j = 1$ when the predictor is included in the good-fitting model j and 0 otherwise.

We could then determine how often a certain predictor was included in the good-fit models. If a predictor was selected more than 50% of the time then it was assigned as a potential for the best-fitting model. Thus, we obtained a 45×17 array (45 glaciers vs. 17 predictors) that consisted of 1 when the predictor was included in the best-fit model and 0 otherwise.

Then, we classified the glaciers in groups. There were a large number of possible combinations to select such groups. Therefore, we constructed a test that assessed every possible combination and calculated a percentage of similarity between glaciers in a group (Eq. 22).

$$S = \frac{M}{17} \times 100, \quad (22)$$

where M is the number of matches between sets of predictors for two glaciers and S is a group number.

Finally, we found that we could categorised all 45 glaciers in 4 different groups, with Group 1 having glaciers/ice shelves that can be more easily combined and Group 4 being a more narrow group of specific glaciers/ice shelves that can not be placed in any of the other three groups.

there should be a i in the riht member?

The Jensen-Shannon Divergence method (JSD) (Dagan et al., 1997) can be used as a tool to measure the distance between two distributions and can provide a value that we can use to assign a particular glacier/ice shelf to one of the groups. The JSD formula is widely used in statistics to measure a divergence of one probability distribution from another. We applied JSD to identify the similarity between the best probability for each glacier and a probability calculated by placing the glacier in a certain group.

The Kullback-Leibler divergence (Kullback and Leibler, 1951) is defined as:

$$JSD(P_1||P_2) = \frac{1}{2} D(P_1||M) + \frac{1}{2} D(P_2||M), \quad (23)$$

where two conditional PDFs $D(P_1||M)$ and $D(P_2||M)$ are defined as:

$$D(P_1||M) = \sum \left(P_1 \log \left(\frac{P_1}{M} \right) \right) \quad (24)$$

and

$$D(P_2||M) = \sum \left(P_2 \log \left(\frac{P_2}{M} \right) \right), \quad (25)$$

where $M = \frac{P_1+P_2}{2}$ and P_1 and P_2 are the new probability (when assigning a glacier/ice shelf to a new group) and the old probability (the best-fit model), respectively. Both probabilities P_1 and P_2 have to be normalised before applying Equation 23.

4.5 Calculation of Damage

Here we utilise the damage-based model as an independent method in order to compare it with our statistics-based method. We do not compare our probability-based model with the damage model directly; rather, we evaluate their respective ability to predict the formation of fractures in ice. For this we compare calculated damage with the observations of fractures and identify areas where it can and cannot accurately predict the presence of fractures.

The Continuum Damage Mechanics approach, based on the method suggested by Kachanov (1958), includes estimation of damaged zones where the ice is softened due to the presence of fractures. Continuum Damage Mechanics has been successfully applied to a wide range of engineering problems as well as to model damage at individually selected ice shelves such as the Ross, Filchner-Ronne, Amery (Bassis and Ma, 2015), Larsen C (Borstad et al., 2013) and Larsen B (Borstad et al., 2016) ice shelves.

Damage is a scalar variable used to determine failure of ice and the nucleation of fractures, usually when the damage predictor reaches a certain value. There are two different methods **for inverting for damage**: methods applied to invert for damage and methods used to model damage propagation in ice sheet models. Borstad et al. (2012) suggested a direct inversion

the second part of the sentence is not restricted to inversion?

for damage using a cost function. Later, Borstad et al. (2013) proposed a method to calculate damage as a post-processing routine after inverting for the ice viscosity. In the first stage, inversion of ice rheology is performed following Larour et al. (2005), then damage is calculated from the inversion of velocities at the ice shelves, which is based on minimising the cost function that quantifies the misfit between the observed and modelled surface velocities.

5 The second stage includes the propagation of damage. Krug et al., 2014; Albrecht and Levermann, 2014) proposed to model the propagation of damage using an advection scheme and a source function. The main limitations of this method are the choice of what should be used as a source function as well as the number of decisive parameters that define the damage evolution (damage threshold, initiation threshold and the enhancement factor). The source function is the controlling factor in the damage propagation and Pralong et al. (2003) as well as Krug et al. (2014) proposed a source function definition. Both
10 of the approaches work well for particular regions, but control predictors in this model have been derived using data from only one specific glacier in Greenland (Duddu and Waisman, 2012) and through the use of small-scale laboratory experiments (Pralong and Funk, 2005) and have not yet been generalised to be applicable to all ice shelves/glaciers. These models do not yet account for factors such as ice fabric and impurities (Borstad et al., 2012).


Recently, Borstad et al. (2016) proposed a framework where, instead of computing a damage source term as is usually done,
15 damage is part of a generalized constitutive relationship. This approach has a number of advantages as it allows the calculation of mechanical ice weakening and the prediction of the degradation of ice shelves. This can significantly improve the accuracy of identifying zones where the ice is weakened by illuminating the uncertainties related to the source function. The main weakness of the approach lies in determining the constant parameters that define damage, because the validity of the parameter values can only be tested when an ice shelf undergoes pronounced mechanical changes, as did the Larsen B Ice Shelf in 2002.
20 The parameters suggested by Borstad et al. (2016) have not been tested for other ice shelves apart from Larsen B, and so it is unknown whether the approach is valid for other locations and settings.


In this study we use the damage inversion method proposed by Borstad et al. (2013) to identify regions where fractures are initiated. Damage in this context has no vertical coordinate, but comes from a linear mapping of the depth-integrated shallow-shelf equations. This approach is performed in two steps. First, the inversion of rheology based on the misfit between observed
25 and modelled velocity is performed on floating ice. Then, damage is calculated as:


$$D = 1 - \frac{B_I}{B_T}, \quad (26)$$


where B_I and B_T are viscosity parameters calculated from an inversion and initialisation of viscosity based on temperature analysis, respectively.


It is important to keep in mind that the inversion only infers damage in areas where fractures (crevasses or rifts) are being
30 actively formed and, thus, creating a jump in strain rate/velocity. Many rifts are formed at one point in time and then only intermittently propagate. If the velocity observations do not show a discrete jump across a fracture, then there is nothing for the inversion to pick up in terms of damage. It only finds fractures that are actively enhancing the flow and it is not meant to locate every fracture.

 Nombre : 1 Auteur : ogagliardini Sujet : Texte surligné Date : 25/08/2018 20:34:11
the second stage of what? Is that in link with the two obove mentioned method?

 Nombre : 2 Auteur : ogagliardini Sujet : Texte surligné Date : 25/08/2018 20:33:26

 Nombre : 3 Auteur : ogagliardini Sujet : Texte surligné Date : 25/08/2018 20:34:44
of crevasses, not damage

 Nombre : 4 Auteur : ogagliardini Sujet : Texte surligné Date : 25/08/2018 20:36:23
are you sure that these two references are not inverted?

 Nombre : 5 Auteur : ogagliardini Sujet : Texte surligné Date : 25/08/2018 20:36:05
Is that the main limitation?

Estimation of B_T is the source of the main uncertainty in damage calculations due to the lack of ice temperature data, which can be crucial in affecting the accuracy of the viscosity parameter (Bassis and Ma, 2015). Thus, the errors in assumed temperature may affect the inferred value for damage.


Fractures that have been advected can be identified by damage but this is not always the case, due to the fact that the inverse method for calculating damage will only find damage where there are fractures that give rise to velocity gradients. Damage will capture some fractures that were formed upstream and advected to a region with different stress conditions only if the fracture enhances the flow and creates a local velocity gradient. Thus, we first calculate flow lines for each observed fracture. If upstream from the fracture the damage is larger than 50% we assume that the observed fracture was formed upstream, that the damage calculation may be correct and that the observed fracture was formed upstream. If there is no damage initiated at the point or damage upstream from the observed fracture we assign the observation point as not captured by the damage method and consider this as a failure of damage to identify the fracture (which can be due to the fact that the fracture in observation point does not cause a local gradient in strain rate).


Physics-based methods, such as Linear Elastic Fracture Mechanics (LEFM) and Continuum Damage Mechanics (CDM), are necessary when modelling fractures in Antarctica. We do not intend to substitute these methods; rather, we seek a method that can improve on some aspects and cases when physics-based models do not predict well the formation of fractures. In particular it is possible that some fractures are initiated upstream from the grounding line rather than on floating ice. It is therefore important to be able to predict the formation of fractures in both cases. Damage is calculated only on floating ice based on model inversions using the Ice Sheet System Model (ISSM) (Larour et al., 2012) because it is not possible to distinguish between basal friction and damage on grounded ice, as they have similar effects on the ice velocity. Thus, the main motivation of this study is not to replace the damage approach, which in fact provides a strong physical background for ice sheet modelling, but to find an alternative method that can be applied to both ice shelves and grounded ice, can work for a large set of glaciers/ice shelves and does not depend on temperature observations and threshold parameters.

5 Results

We applied the LRA method combined with the random walk method to 45 ice shelf regions that include both ice shelves and surrounding grounded ice (the corresponding names and locations can be found in Table 6 and Figure 3a, respectively) and found a best-fitting model for 44 of them. The fracturing of the remaining ice shelf cannot be described using the predictors we have, producing unacceptably large or small probabilities.

In total, for each ice shelf/glacier the random walk analysis gave a number of possible sets of predictors that can produce a good-fitting model. We combined all of these possible sets for each glacier to see which predictors are always present in the good-fitting model and which ones are never included. The results of the random walk and the Bayesian inversion agreed well. Most of the essential predictors for each particular glacier selected in the Bayesian approach were also chosen when performing the random walk. In most cases, the Bayesian analysis showed equal importance of most of the predictors although effective strain rate and velocity had a slightly higher rate of selection. There was no universal set of factors that could be used to model

 Nombre : 1 Auteur : ogagliardini Sujet : Texte surligné Date : 25/08/2018 20:40:47
is the repetition in this sentence necessary?

 Nombre : 2 Auteur : ogagliardini Sujet : Texte surligné Date : 25/08/2018 20:43:40
Fig.
check this everywhere in the manuscript and refer to the TC instructions.

all ice shelf regions. However, subsets of glaciers had some similarities in terms of the predictors that had to be included in order to achieve a good-fitting model.


To estimate how well our probability model and the damage model identify observed fractures we calculated the percentage of success and error for each ice shelf/glacier model. First, we found the number of cases when there is a modelled fracture in the vicinity of an observed fracture (within 100-metres radius). Then, we divide this number by the total number of observed fractures to find the percentage of success. To find the percentage of failure we calculated how many times there is a modelled fracture when there are no observed fractures within a 100-metres radius. We divide this number by the total number of non-fractured nodes to find the failure percentage.

Thus, we categorised the 45 glaciers into 4 groups, requiring that the deviation from the best-fit models did not exceed 5%.


Next, we performed a test to assess whether these selected sets were the optimal choice, by estimating the deviation from the best solution using the Jensen-Shannon Divergence algorithm. We assigned each glacier to a particular group based on its minimum value of the deviation from the best-fitting model in JSD analysis. In so doing, we slightly modified the members of each group that we had previously created. For example, Glacier 27 belonged to Group 1 previously and it fit well with only a slight change of the best-fit score. However the JSD showed that if we move this glacier to Group 2 the deviation from the best-fit decreased from 0.01 to 0.003. However, we had to take into account the fact that the JSD algorithm measures the total distance to the best-fit probability and, thus, can decrease the over-estimation error while, at the same time, significantly decrease the success rate (Glaciers 10, 13, 15, 11, 30, 32). Therefore, since these six glaciers were of a similar type to the glaciers in Group 1 and their JSD was similar for Group 1 and Group 2 (e.g JSD=0.02 in Group 2 and JSD=0.0205 in Group 1) they were assigned to Group 1 to avoid a decrease in the success rate of identifying fractures.

Finally, to reach an optimal agreement between our model and the observations of fractures, we assigned each glacier to a particular group and the set of factors for each group are presented in Table 3 and Table 4, 5, respectively. We found that the sets of predictors for each group varied significantly, however surface velocity was included in the grounded ice set for all groups. For the floating ice the analysis showed that surface velocity was not a determining factor in predicting fractures, instead effective strain rate as well as deviatoric principal stress values were present in each predictor set.

While the success of identifying fractures on floating ice was lower than for grounded ice, we were still able to identify the main fracture patterns and the success rate was high for the majority of ice shelves (see Figure 2a). Our method is able to identify up to 99% of the exact location of fractures on grounded ice with an average of 84% (Figure 2a) and 61% for floating ice (Figure 2b). The mean over-estimation error for grounded ice and floating ice was 26% and 20%, respectively. There are many cases where our method agrees with the results produced by the damage-based approach. However, in almost all cases the success of LRA on floating ice was higher than of the damage-based method with the exception of two glaciers. Overall, for all four groups, where we could not achieve a high score using LRA, the damage-based method did not produce a high success score either (see Figure 2b).

 Nombre : 1 Auteur : ogagliardini Sujet : Texte surligné Date : 25/08/2018 20:46:47
don't understand the list of glaciers here and its link to the sentence. Explain.

 Nombre : 2 Auteur : ogagliardini Sujet : Texte surligné Date : 25/08/2018 20:47:50
in Tables 3, 4 and 5

 Nombre : 3 Auteur : ogagliardini Sujet : Texte surligné Date : 25/08/2018 20:55:41
It was correct in the previous version, should be Fig. Refer to https://www.the-cryosphere.net/for_authors/manuscript_preparation.html

5.1 Group 1


This was the largest group of glaciers and the best-fit model includes as many as 10 predictors for grounded ice and seven predictors for floating ice. The analysis of the estimated coefficients in LRA showed that predictors with the highest weights in our model for this group of glaciers were: effective strain rate, proximity to glacier edges and nunataks as well as the surface elevation gradient. We present the modelled probability of fractures in **Figures 5b and 4c** as well as comparison with the damage-based results in Figures 7a and 10c.


The main pattern of surface fractures is well represented for this group. On grounded ice the success of identifying fractures is larger than 88% with a quarter of glaciers at almost 100%. The failure related to over-estimation of fractures is 27%. On floating ice the success amounted to 55% and the failure was equal to 15% on average. For **Randerford IS** (see Figure 5b) the overall pattern is well represented, even though high resolution images were not available for this glacier. The over-estimation error is mainly related to the region that is far from the ice front and has a relatively high accumulation rate, possibly obscuring the fractures in the imagery. On floating ice the probability of fracturing is relatively smaller, mainly showing a higher chance of fracturing closer to the grounding line. Conversely, Drygalski Ice Shelf has a larger number of high resolution areas and, as a possible result, less over-estimation of fracturing (see Figure 4c). We can see that the “definitely non-fractured nodes” (selected in blue ice areas) are successfully represented in our model. For this glacier, none of the observed non-fractured nodes was assigned to have a high probability of fracturing, with the modelled probability being as low as 0.1. Moreover, in the regions with a large number of observed fractures, the probability is as high as 0.9 and it is slightly lower in the areas with a smaller number of observed fractures (between 0.6 and 0.8). Observed fractures not captured by our model were not captured by the damage-based model either.

The modelling results for the Cook ice shelf are shown in Figure 7b. There are distinct fractures visible towards the front and in the central part of the ice shelf that are not captured by either approach, which we interpret as showing that most of the fractures are formed further upstream near the grounding line. In general, the probability and the damage-based models show good agreement on the floating ice near the grounding line. However, damage does not reach 50% in the majority of the locations. Moreover, in many locations where rifts are visible it shows 0 damage.

The modelling results for Larsen B IS are illustrated on Figure 10c. It is clear that the nodes where damage is high have a high probability of fracturing due to the fact that we added damage as one of the predictor parameters to this glacier. It can be also seen that there are two lines of high probability of fracturing that coincide with the location of the large rifts that can be seen on the satellite images.

The results for Nansen IS (Figure 8c) as well as for Pine Island (Figure 6a) agree well with observations even though the data from these two glaciers were not included in the calibration data set used to construct the LRA model. For Pine Island, we observe fractures in the central part of the shelf that were not captured by the model, but our model predicted high probabilities of fracture upstream where the ice is grounded. Thus, these fractures are likely advected from the grounding line out onto the floating ice shelf.

 Nombre : 1 Auteur : ogagliardini Sujet : Texte surligné Date : 25/08/2018 20:56:22
Figs.

 Nombre : 2 Auteur : ogagliardini Sujet : Texte surligné Date : 25/08/2018 20:57:13
give its number also?

6.5 Discussion

We found that, in general, the most important predictor factors to model surface fractures on grounded ice for all analysed glaciers were the surface velocity and the change of the surface gradient, which is in agreement with the theory of possible mechanism of fracture formation (Colgan et al., 2016). Interestingly, the required parameters on floating ice were different from grounded ice, with effective strain rate and principal stress being the most important. Previous analysis based on damage accounts for effective stresses, thickness and viscosity, but does not include such predictors as proximity to glacier edges, nunataks and the grounding line as well as the curvature of a channel, which helped to improve the modelling of fractures on most ice shelves in our analysis. Our results can be used to identify potential regions with snow covered crevasses that may pose hazards for navigation in Antarctica. Many researchers use ground penetrating radar to find hidden crevasses, but it is a real time assessment method that requires both financial and human resources and, therefore, can not cover all the areas in Antarctica. Our approach can be done remotely and at low cost, in advance of field campaigns.

We do not claim that all the predictors that were chosen in the final set for each group represent the exact fracture mechanisms for each glacier. For some ice shelf regions, sets containing different predictors can lead to results close to the best-fitting model. However, for some cases, such as Amery and Totten Ice Shelves the number of good-fitting models is very limited. For example, including the effective strain rate and proximity to the ice front in the analysis we can achieve a better fit to the observations. Therefore, we conclude that some factors have a very strong effect on fracturing, while others are only minor for some glaciers. Ultimately, we seek only to be able to develop a model that can identify correctly the geographical location of fractures, not necessarily explain why they are there.

The main uncertainty of our method is related to the over-estimation of the number of fractures. It could be argued that we predict fractures in the locations where no observations of fractures are detected due to the fact that they are not visible due to snow accumulation or coarse resolution. A possible solution to this could be to supplement satellite images with radar and seismic measurements (Navarro et al., 2005; Delaney and Arcone, 2005) or to acquire higher resolution satellite images that can help to identify location of fractures even if they are hidden under the snow surface. However, for our method it would require a large set of observational data. In our paper we assume that 20-25% rate of over-estimation is reasonable, since most of our results show over-estimation when predicting fractures in the areas around observed fractures. Our assumption is based on the fact that the ice regime conditions are similar within a 500 metres radius, not implying any direct influence of the old fractures to the new fractures (Colgan et al., 2016). In addition, the area of high probability of a fracture is larger than the number of observed fractures mainly due to the fact that it is not possible to select all of the fractures on the satellite images manually. The observed fractures in our evaluation data set capture the main areas of fracturing assuming that surrounded nodes are likely to be fractured as well.

A significant over-estimation of predicted fracturing can be seen at the front of Vanderford IS (see Figure 5b), suggesting that there is a very high chance of developing surface fractures in that area. It may be that fractures exist there that are just not visible on the satellite images. In fact, that region has a relatively high snow accumulation rate reaching 1 m/yr. After closer inspection of the satellite image areas where we see the over-estimation error, we can recognise the presence of surface

is this paragraph at the right place. At most place, radar is used for security, as crevasses evolve from on year to an other, so that I am not convince your method could completely replace the instantaneous filed measurement.

fractures and we may have under-identified existing fractures in that area. Due to a very large number of fractures around Antarctica, the manual selection of all the fractured data points is a time intensive process. Sampling with a higher spatial density would require an automated algorithm. However, the low spatial density sampling does not influence the results of the fracture probability (as mentioned previously only diversity in sampling is important), it affects only the observations data set that we use to estimate the success of our model. Thus, under-identification of fractures can lead to an apparent over-estimation of the error.

The damage-based approach sometimes produces areas of high damage downstream of the observed fractures (Figure 9d). If we assume that there are some fractures that are not visible on the images it is still unclear why the modelled ice is not damaged upstream where observed fractures are present. If we could see damaged ice upstream from the observed fractures we could assume that the ice was damaged and transported downstream where we can see fractures. However, in many results based on the damage approach we could not identify this type of behaviour. Even after correcting the observations of fractures by back integrating the flow of ice, we still can find fractures that do not have zones of high damage upstream of the fractures. In addition, the method based on damage inversion predicts only damage on floating ice, whereas fractures are often formed upstream of the grounding line. In our probability-based model this type of behaviour is accounted for and the model in most cases overestimates fractures only in the vicinity of or upstream of observed fractures. In Figure 8a we show modelled probability of fracturing for Holmes IS. The over-estimation rate is quite small and it all occurs upstream of the observed fractures, which might be due to fractures that were formed further upstream being transported downstream where they are visible on the satellite images.

We looked at various properties of Ronne IS for which we could not find a good approximation using any of the 17 predictors. We found that the Ronne IS has the lowest elevation change as well as the principal stresses components. We do not have enough samples to cover values that are non-typical for the majority of glaciers, which may explain why we could not find a good-fit model for this ice shelf, neither with LRA nor using the Bayesian analysis. Thus, we conclude that our probabilistic model is not appropriate in this case.

7 Conclusions

Most previous large-scale modelling of surface fractures has focused on applying zero stress, Linear Elastic Fracture Mechanics, Continuum Damage Mechanics. We have shown that, using the suggested nominal parameters, damage-based approach does not fully reproduce the location of fracturing for any ice shelf region. In this study, we constructed a probability-based method to model surface fractures and generated improved predictions of fractures when physics-based models did not predict well the location of surface fractures. From this different perspective, we can construct an alternative method to predict the location of fractured zones not only on floating ice but also on grounded ice.

We found that the Logistic Regression Analysis, combined with other statistical methods, can significantly improve the prediction of fractured zones for the Antarctic ice shelves/glaciers and can lead to the identification of up to 99% of observed surface crevasses for some ice shelf regions with an average of 70% for all ice shelf regions. Our approach has a number of

8 Tables

Table 1. Development of calving parameterisations

Year	Reference	Method
1955	Crevasse penetration depth using tensile stress and overburden pressure	Nye (1955)
1973	Crevasse penetration depth of a single crevasse	Weertman (1973)
1976	Crevasse penetration depth estimation using LEFM	Smith (1976)
1993	Strain related fracture formation	Vaughan (1993)
1997	Sea level dependent calving	Motyka (1997)
1998	Linear Elastic Fracture Mechanics	Van der Veen (1998a, b)
2003	Damage mechanics for a single crevasse	Pralong et al. (2003)
2005	Damage mechanics for a single crevasse	Pralong and Funk (2005)
2007	Crevasse depth	Benn et al. (2007a, b)
2010	Crevasse depth	Nick et al. (2010)
2010	Crevasse depth	Otero et al. (2010)
2012	Damage mechanics applied to a crevasse field	Borstad et al. (2012)
2012	Kinetic 1st order calving	Levermann et al. (2012)
2012	CDM	Duddu and Waisman (2012)
2013	CDM	Duddu and Waisman (2013)
2013	Discrete element models	Bassis and Jacobs (2013)
2013	Particle-based simulation	Astrom et al. (2013)
2013	Crevasse depth criterion	Nick et al. (2013)
2014	Crevasse depth criterion	Cook et al. (2014)
2014	CDM	Albrecht and Levermann (2014)
2014	Combining CDM and LEFM	Krug et al. (2014)
2016	von Mises tensile stress	


Table 2. Predictor factors (predictors)

Type	Predictor	Description
Geometry	Ice thickness	Bedmap2 data for Antarctica at 1 km spatial resolution
	Maximum bed slope	Bedrock and ice surface slopes are ¹ calculated using a nodal function
	Maximum surface slope	
	Proximity to the ice front	DM_{IF} , calculated using Eq. 9
	Proximity to grounding line	DM_{GL} , calculated using Eq. 10
	Proximity to glacier edges and nunataks	
	Curvature	Curvature of the glacier channel α , calculated in each node based on the direction and rate of the flow velocities (see Eq. 11)
Flow parameters	back stress	Buttressing effect on ice streams calculated in ISSM from inversion
	Velocity	InSAR ice flow velocity
	Rheology predictor (viscosity)	B , Glen's flow predictor, calculated from inversion of velocities (only for floating ice)
	Effective Strain rate	The effective strain rate is calculated using Eq. 8 with observed velocities as an input
	Principal stress (1 and 2)	² eigenvalues λ (normal stresses) in Eq. 4
	Principal strain rate (1 and 2)	Eigenvalues μ (see Eq. 7)
	Strain rate gradient	Maximum strain rate change in a 400-600 metres vicinity

Table 3. Formed groups of ice shelf regions

Group1	9, 10, 11, 12, 13, 15, 18, 20, 21, 23, 25, 26, 30, 31, 32, 34, 4, 29
Group2	3, 6, 7, 8, 19, 27, 28, 33, 35
Group3	14, 17, 22, 24
Group4	1, 2, 5, 16

Glaciers/ice shelves for which we could not find a good-fitting probability are marked with red.

 Nombre : 1 Auteur : ogagliardini Sujet : Texte surligné Date : 25/08/2018 23:01:42
which dataset?


 Nombre : 2 Auteur : ogagliardini Sujet : Texte surligné Date : 25/08/2018 23:02:04
from what?

Table 4. Predictors for grounded ice regions in each formed group

	Effective stress	Effective strain rate	Principal 1 strain rate	Principal 2 strain rate	Principal 1 stress	Principal 2 stress	Surface slope	Bed slope	Strain change	Curvature	Rheology B	Thickness	at the ice front	at the grounding line	near edges	surface change	Velocity
Group1:		✓	✓				✓			✓	✓		✓		✓	✓	✓
Group2:	✓				✓				✓		✓	✓				✓	✓
Group3:				✓								✓			✓		✓
Group4:		✓							✓	✓						✓	✓

Tick-mark stands for an addition of a predictor to the model for grounded ice.

Table 5. Predictors for floating ice in each formed group

	Effective stress	Back stress	Effective strain rate	Principal 1 strain rate	Principal 2 strain rate	Principal 1 stress	Principal 2 stress	Surface slope	Strain rate change	Curvature	Rheology B	Thickness	at the ice front	at the grounding line	surface change	Velocity
Group1:	✓				✓	✓		✓	✓							✓
Group2:			✓			✓					✓	✓		✓	✓	
Group3:			✓				✓				✓	✓			✓	
Group4:		✓	✓	✓				✓	✓					✓	✓	✓

Tick-mark stands for an addition of a predictor to the model for floating ice.

why only putting a mark and not the derived beta value for each predictor? It would give information on which predictor are the most important in each group.

What is the beta threshold value to have a mark or not?

Table 6. A list of analysed ice shelf regions

Glacier	Group	Corresponding IS name	Region
1	4	George IV	Palmer land, AP
2	4	Larsen C	Fallieres Coast, AP
3	2	Larsen D	Black Coast, AP
4	1	Orville Coast side of the Ronne IS	WA
5	4	Amery	EA
6	2	Edward VII	Mawson Coast, EA
7	2	Rayner Thyner	EA
8	2	Shirase	Prince Harald Coast, EA
9	1	Stancomb-Brunt	Caird Coast, EA
10	2	Riiser-Larsen	Princess Martha Coast, EA
11	3	Fimbul IS	EA
12	1	Abbot	Eights Coast, WA
13	2	Baudoin	Princess Ragnhild Coast, EA
14	3	Nivl	Princess Astrid Coast, EA
15	1	Borchgrevnik and Lazarev	Princess Astrid Coast, EA
16	4	Borchgrevnik	Princess Raghild Coast, EA
17	3	Dibble IS	Clarie Coast, EA
18	1	Mertz IS	EA
19	2	Rennik	Pennell Coast, EA
20	1	Cook	George V Coast, EA
21	1	Ninnis	George V Coast, EA
22	3	Holmes	Banzare Coast, EA
23	1	Moscow University	Sabrina Coast, EA
24	3	Totten IS	EA
25	2	Vanderford IS	EA
26	1	West IS	Queen Mary Coast, EA
27	2	Larsen C	Oscar II Coast, AP
28	2	Larsen B	Nordenskjold Coast, AP
29	2	Larsen A	Davis Coast, AP
30	3	Tracy-Tremenchus	Knox Coast, EA
31	1	Drygalski	Scott Coast, EA
32	2	Mariner	Borchgrevnik Coast EA
33	3	Rennik	Lazarev Mountains, Oates Coast, EA

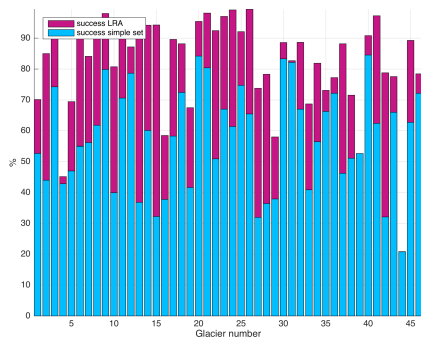
Is it discussed in the text that the analysis for Ronne IS is restricted to this area?

From the text, the reader is expecting a line in this table for Ronne IS with no group assigned.

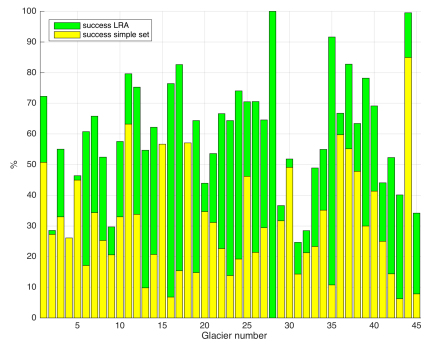
Table 7. A list of analysed ice shelf regions

Glacier	Group	Corresponding IS name	Region
34	1	Filchner	Coast Land, WA
35	2	Ross East	Hut Point Peninsula, EA
36	1	Wilkins and George VI	Rumill Coast, AP
37	1	Stange and Ferringo IS	Bryan Coast, AP
38	1	Pine Island and Thwaites	Walgreen Coast, WA
39	2	Getz	Hobbs and Bakutis Coast, WA
40	1	Nickerson and Sulzberger	Ruppers Coast, WA
41	1	West	Leopold and Astrid Coast, EA
42	1	Jelbart and Atka	Princess Martha Coast, WA
43	1	Nansen	Borchgrevnik Coast, EA
44	1	Prince Harald	Prince Harald Coast, EA
45	1	Larsen B	Oscar II Coast, AP

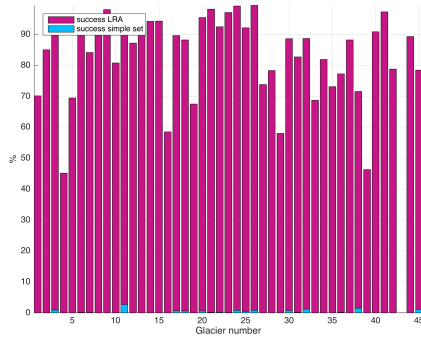
AP - Antarctic Peninsula, EA - East Antarctica, WA - West Antarctica, IS -ice shelf



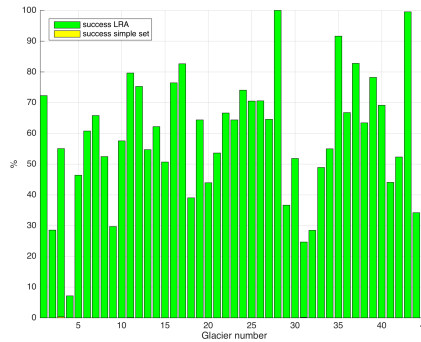
(a) Grounded ice, final set vs test set 1



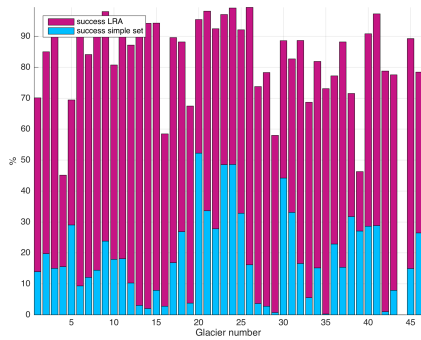
(b) Floating ice, final set vs test set 1



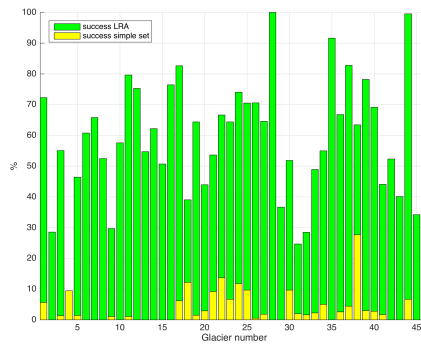
(c) Grounded ice, final set vs test set 2



(d) Floating ice, final set vs test set 2

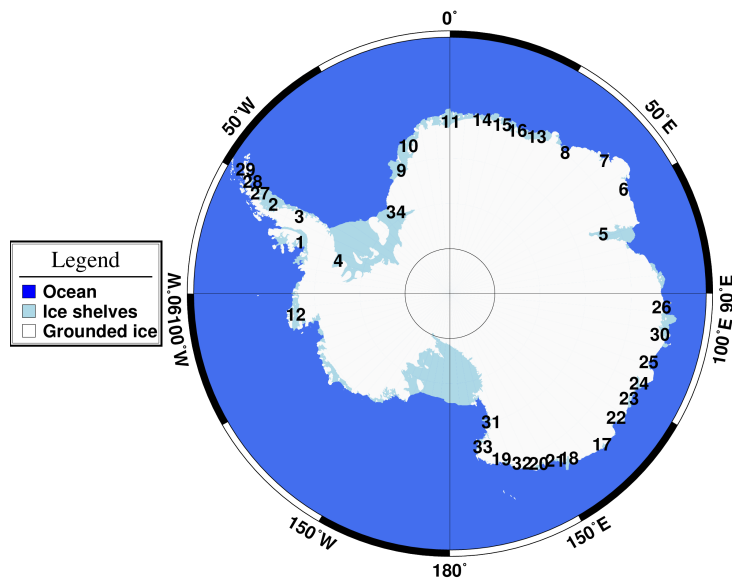


(e) Grounded ice, final set vs test set 3

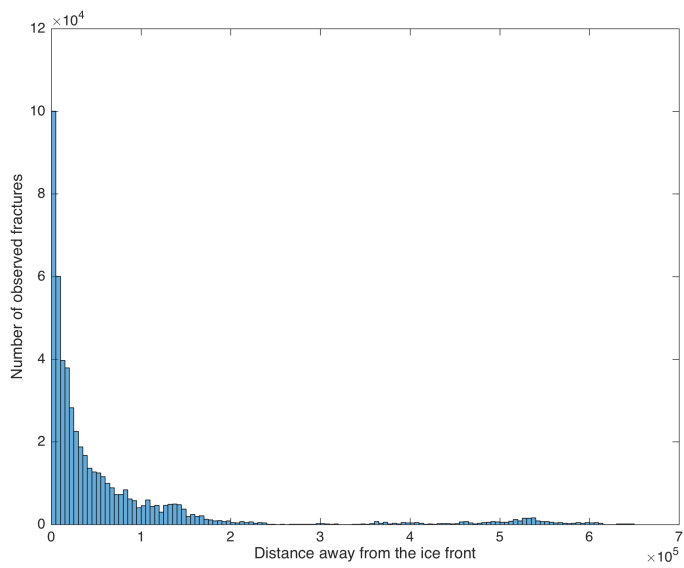


(f) Floating ice, final set vs test set 3

Figure 1. Comparison between the success of identifying fractures using LRA (purple for grounded ice, green for floating ice) and using Test set 1: effective deviatoric stress, Test set 2: principal deviatoric stress 1 and 2, Test set 3: von Mises stress (blue for grounded ice, yellow for floating ice). Left column represents grounded ice (a,c,e) and right show the results for floating ice (b,d,f).



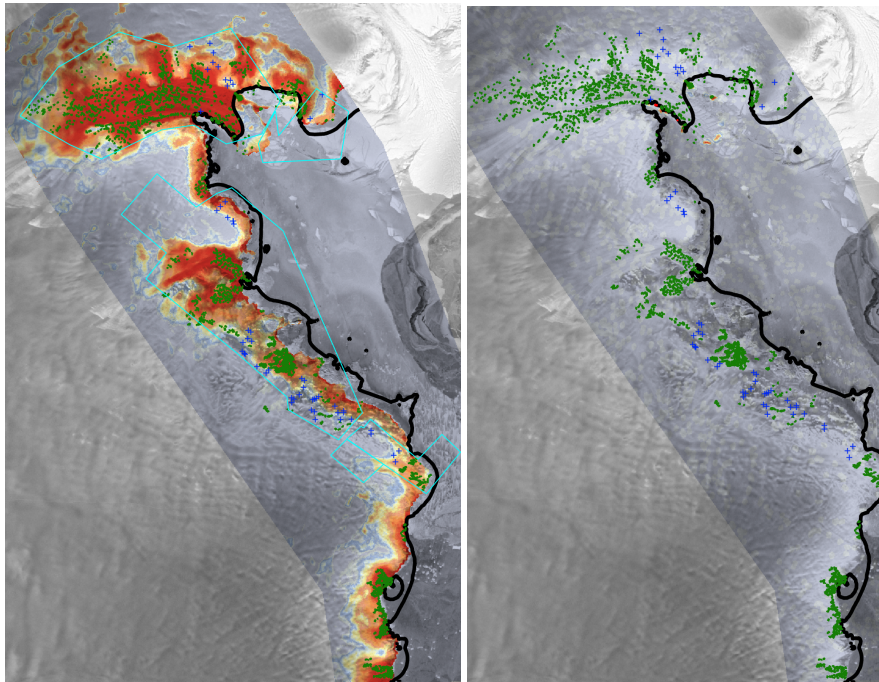
(a) Location



(b) Distance to the ice front

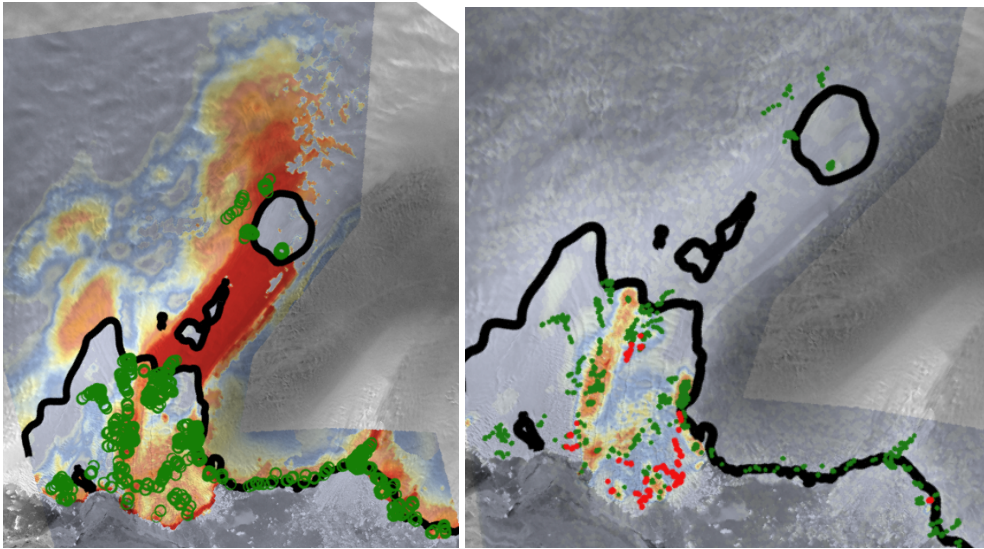
Figure 3. The location of each of the 45 ice shelf regions is shown in panel a. The number of observed fractures versus distance from the ice front (b).

What is the reason to have these two panels in the same figure?



(a) LRA, Shirase IS

(b) Damage, Shirase IS



(c) LRA, Totten IS

(d) Damage, Totten IS

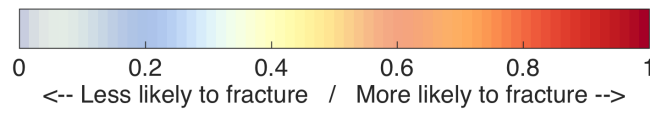
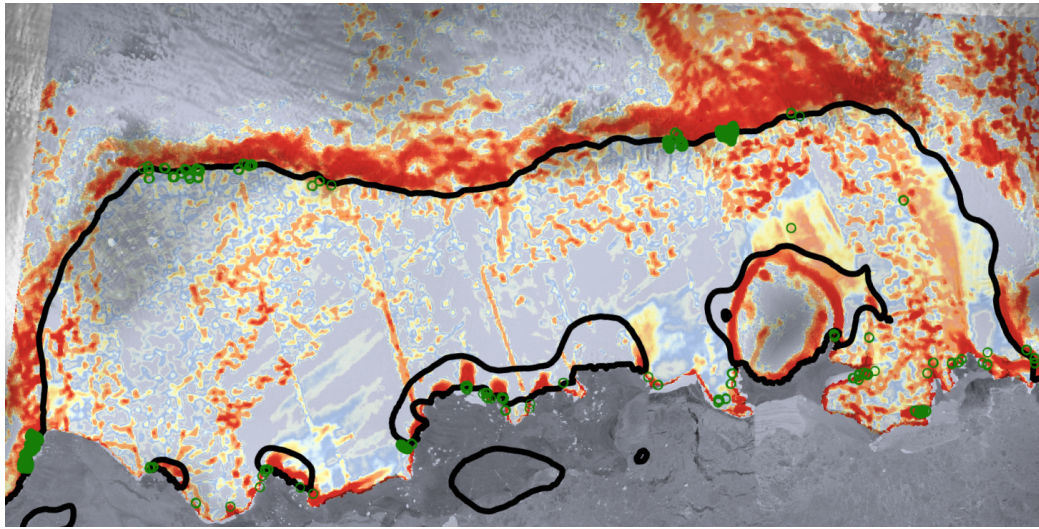
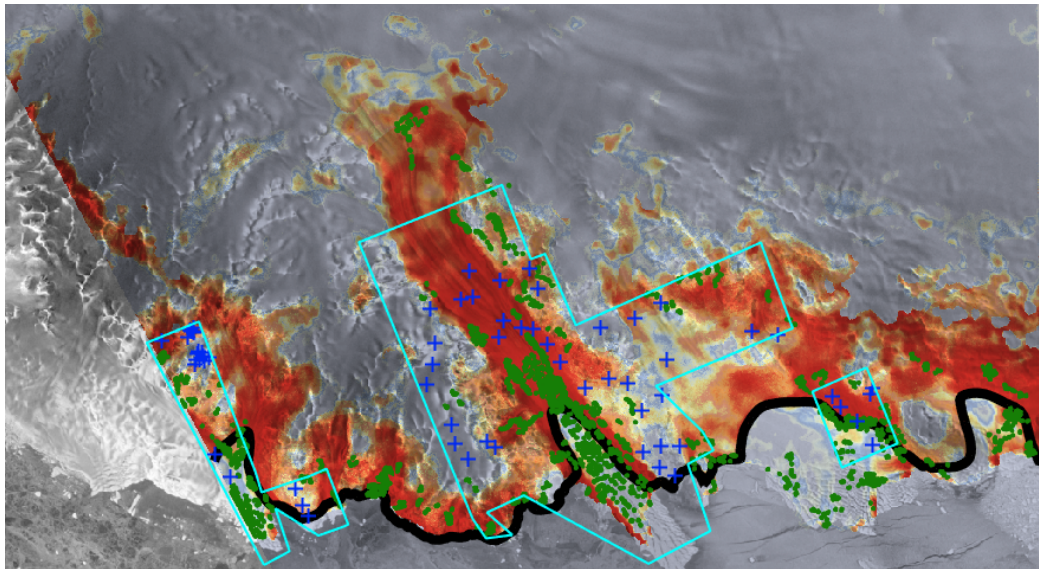


Figure 11. Modelled probability of a fracture vs. modelled damage for Shirase IS (Group 2) (a, b) and Totten IS (Group 3) (c, d). Labels are the same as in [figure 4 and 7](#).



(a) Baudoin IS, Group 1



(b) Rennik IS, Group 1

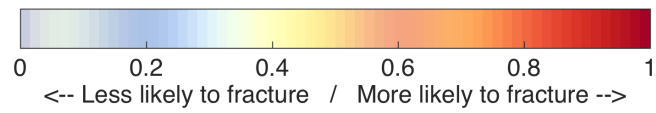
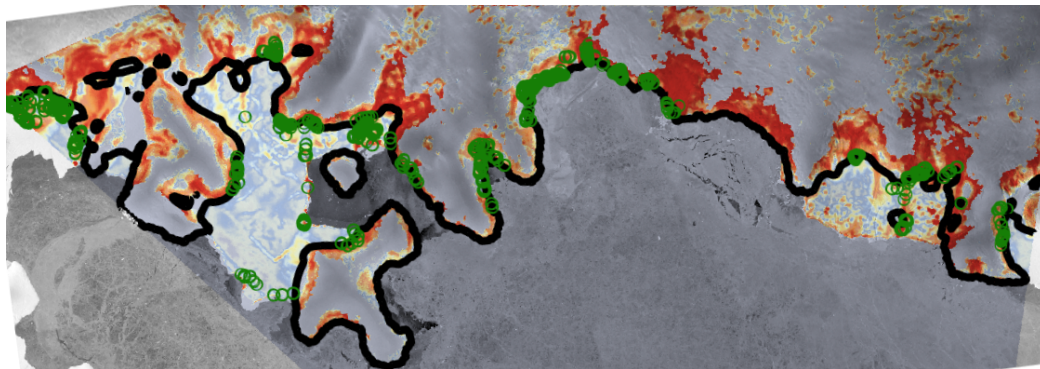
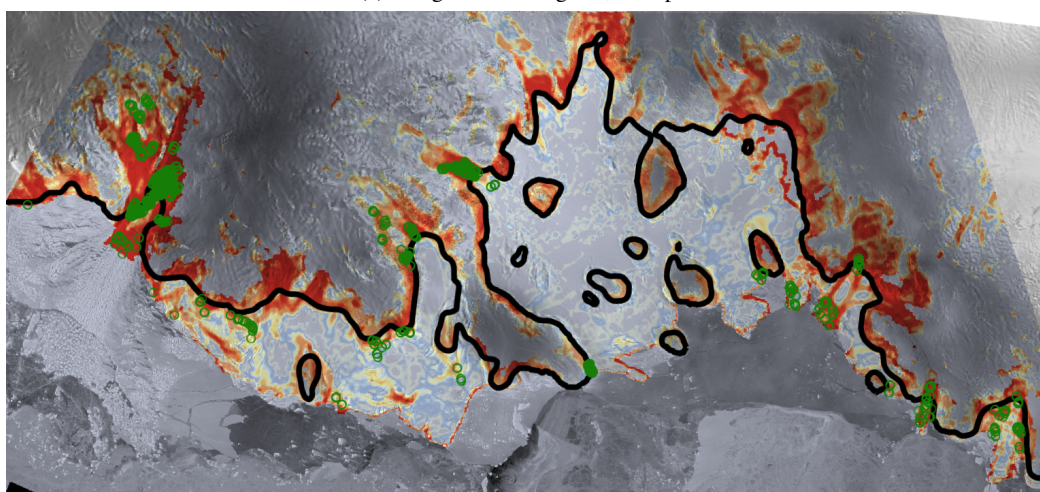


Figure S1. Group 1: Modelled probability of a fracture for Baudoin IS (a) and Rennik IS (b). Observed surface fractures are shown in black and observed non-fractured ice is marked with orange circles. Red polygons represent regions where high resolution images were available.

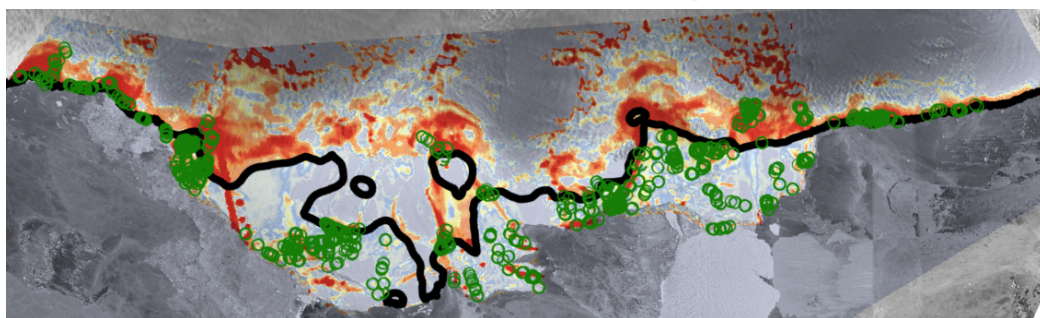
I was not able to find a reference to these S1 to S8 figures in the text. Check that all figures are cited in the text.



(a) Stange and Ferringo IS, Group 1



(b) Nickerson and Sulzberger IS, Group 1



(c) West IS, Group 1

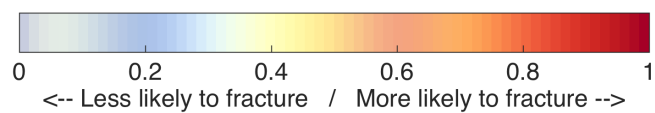


Figure S8. Group 1: Modelled probability of a fracture for Stange and Ferringo IS (a), Nickerson and Sulzberger IS (b) and West IS (c). Labels the same as [Figure S1](#).

